406 J. Med. Chem. 2011, 54, 406–410
DOI: 10.1021/jm101068q

Journal of Medicinal Chemistry
Brief Article

4-[^{18}F]Fluoroglutamic Acid (BAY 85-8050), a New Amino Acid Radiotracer for PET Imaging of Tumors: Synthesis and in Vitro Characterization

Raisa N. Krasikova,[†] Olga F. Kuznetsova,[†] Olga S. Fedorova,[†] Yuri N. Belokon,[‡] Viktor I. Maleev,[‡] Linjing Mu,[§] Simon Ametamey,[§] P. August Schubiger,[§] Matthias Friebe,*[,∥] Mathias Berndt,[∥] Norman Koglin,[∥] Andre Mueller,[∥] Keith Graham,[∥] Lutz Lehmann,[∥] and Ludger M. Dinkelborg[∥]

[†]*Institute of Human Brain of the Russian Academy of Science, Academika Pavlova 9, St. Petersburg, 197376, Russia,* [‡]*A. N. Nesmeyanov Institute of Organoelement Compounds of the Russian Academy of Science, B-334, Vavilova 28, Moscow, 119991, Russia,* [§]*Center for Radiopharmaceutical Science of ETH, PSI, and USZ, Department of Chemistry and Applied Biosciences, ETH Zurich, 8093 Zurich, Switzerland, and* [∥]*Bayer Schering Pharma AG, Global Drug Discovery, 13342 Berlin, Germany*

Received August 17, 2010

There is a high demand for tumor specific PET tracers in oncology imaging. Besides glucose, certain amino acids also serve as energy sources and anabolic precursors for tumors. Therefore, ^{18}F-labeled amino acids are interesting probes for tumor specific PET imaging. As glutamine and glutamate play a key role in the adapted intermediary metabolism of tumors, the radiosynthesis of 4-[^{18}F]fluoro L-glutamic acid (BAY 85-8050) as a new specific PET tracer was established. Cell-uptake studies revealed specific tumor cell accumulation.

Introduction

The effectiveness of cancer treatment requires powerful diagnostic tools that allow for early detection of tumors and related metastases and for patient staging, stratification, early therapy response assessment, and therapy monitoring. Targeting of tumor specific metabolic pathways represents a useful strategy for early tumor detection and characterization.

Many tumors show an increased uptake and metabolism of glucose via the Emden−Meyerhof−Parnas pathway even in the presence of oxygen. In the 1920s Otto Warburg recognized and described this altered metabolism of cancer cells by in vitro studies.[1,2] Today, increased uptake of glucose and enhanced glycolytic metabolism of tumors is used for tumor imaging with the fluorine-18 radiolabeled glucose analogue 2-[^{18}F]fluoro-2-deoxy-D-glucose ([^{18}F]FDG, **1**; see Chart 1) by means of positron emission tomography (PET[a]). Radiolabeling with the positron emitter fluorine-18 allows for signal detection by state-of-the-art PET technology, and in addition, the fluorine substitution promotes intracellular trapping of the tracer, as no further metabolism beyond phosphorylation by hexokinase is possible. Thus, the fate of **1** ([^{18}F]FDG) can be followed noninvasively in vivo and has become a valuable tool in clinical routine for PET-imaging of tumors.[3]

Although today **1** is by far the most often used PET tracer worldwide, it has several pitfalls and limitations necessitating development of alternative imaging probes. Glycolysis is enhanced in many tumors, but it is not necessarily a tumor specific pathway. Like glucose, **1** is accumulated in other tissues possessing an increased glycolytic metabolism such as in fast dividing tissues, sites of inflammation, brain, and brown adipose tissue. Therefore, artifacts like increased uptake of **1** in inflamed tissues around tumors after radiation therapy or in scar tissue after surgery make image interpretation and monitoring of tumor therapy difficult or even impossible. Moreover, PET with **1** has limitations in the detection of tumors with low metabolism such as prostate,[4,5] bladder, and renal cancer, tumors of low cell density, small tumors, and other FDG nonavid cancers.[6]

Chart 1. Structures of **1** ([^{18}F]FDG) and **2** ([^{18}F]FET)

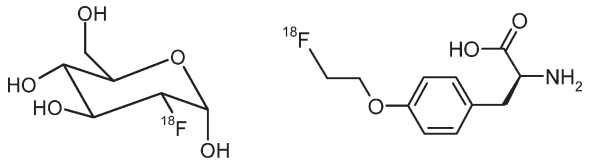

1 [^{18}F]FDG **2** [^{18}F]FET

Besides glucose, tumors also show an enhanced demand for certain amino acids. Therefore, ^{18}F-labeled amino acids could be interesting alternatives for tumor imaging. For example, [^{18}F]fluoroethyl tyrosine ([^{18}F]FET, **2**; see Chart 1) is currently evaluated for the in vivo targeting of brain tumors.[7] In contrast to **1** the specific tumor uptake of **2** ([^{18}F]FET) is accompanied by a low background signal in normal brain tissue. First experimental animal models provided evidence that **2** might be able to distinguish between tumor and inflammatory tissue.

Unfortunately the use of **2** is hampered by its moderate tumor accumulation in peripheral, nonbrain tumor entities and a significant background signal in human subjects.[8−10]

*To whom correspondence should be addressed. Phone: +49-30-46811828. Fax: +49-30-46891828. E-mail: matthias.friebe@bayer.com.

[a] Abbreviations: BPB, (*S*)-[*N*-2-(*N*′-benzylprolyl)amino]benzophenone; BSA, bovine serum albumin; FCS, fetal calf serum; nca, non-carrier-added; PBS, phosphate buffered saline; PET, positron emission tomography; PTC, phase transfer catalyst; TCA, tricarboxylic acid; 4-[^{18}F]F-Glu, 4-[^{18}F]fluoro-L-glutamic acid; [^{18}F]FDG, 2-[^{18}F]fluoro-2-deoxy-D-glucose; [^{18}F]FET, [^{18}F]fluoroethyltyrosine.

 Published on Web 12/03/2010

In fact, the tumor/nontumor tissue ratios for **2** are by far lower than for **1** except within the brain.[8] Therefore, a highly accumulating tumor specific ^{18}F-labeled amino acid tracer is of outmost interest.

It is well-known that certain amino acids serve as major energy source and building blocks for tumors. In particular there is emerging evidence for the existence of a tumor-specific truncated tricarboxylic acid (TCA) cycle associated with a high rate of glutaminolysis and lipogenesis.[11−14] Hence, glutamine and glutamate play key roles in the adapted intermediary metabolism of tumors. After deamidation of glutamine, glutamate is further transaminated to 2-oxoglutarate, which is directly channeled into the truncated TCA cycle, where it is further metabolized in several consecutive reactions to provide energy and building blocks (Figure 1). Therefore, ^{18}F-labeled derivatives of glutamine/glutamate are of particular interest.

Here we report the design of a ^{18}F-labeled glutamate derivative and an efficient radiosynthesis strategy that is a prerequisite for successful preclinical evaluation and a prospect for subsequent clinical studies. The direct introduction of [^{18}F]fluoride via the nucleophilic substitution process of an appropriate leaving group is well established and requires alkaline conditions.[15] However, the stability of the labeling precursor and the preservation of the desired stereoisomeric configuration mark a significant challenge in the stereochemically controlled synthesis of enantiomerically pure ^{18}F-labeled amino acids under such radiolabeling conditions.[16,17] This challenge was addressed by the introduction of precursors with bulky protective groups on the carboxy and amino functions.[16] We recently published a stereoselective approach to generate ^{18}F-labeled tyrosine via direct nucleophilic fluorination using the enantiomerically pure Ni(II) precursor of a Schiff base (*S*)-[*N*-2-(*N*′-benzylprolyl)amino]benzophenone (BPB) with alkylated (*S*)-tyrosine.[17] This methodology was

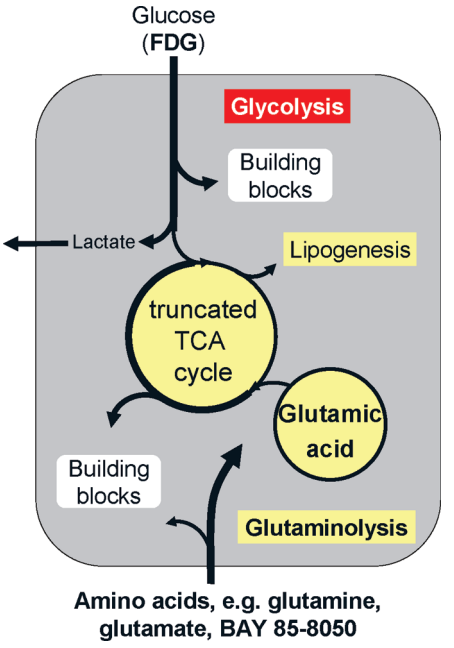

Figure 1. Key roles of glutamine and glutamic acid and specific adaptations of the intermediary tumor metabolism. Glycolysis is not a tumor-specific pathway.

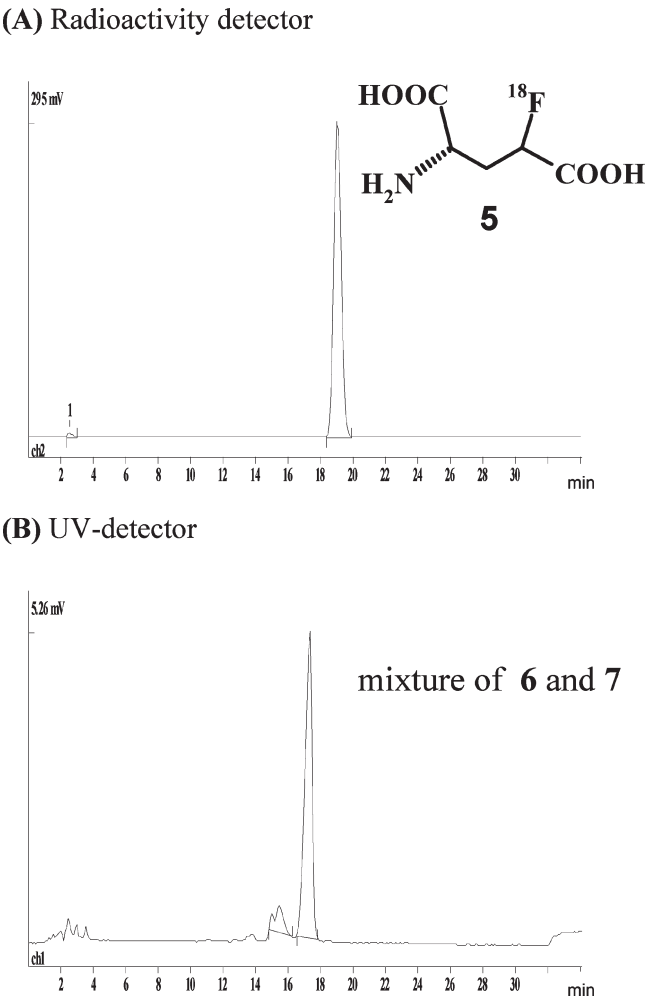

Figure 2. Analytical radiochromatogram of the purified **5** (column Zorbax NH_2, 4.6 mm × 250 mm, eluent 10 mM NaH_2PO_4 (pH 3.5)/MeOH (85/15 v/v), 1.5 mL/min): (A) detection of radioactivity and (B) UV detection at 210 nm (UV detector preceding the radiodetector in a line-setting).

Scheme 1. Radiosynthesis of nca **5**[a]

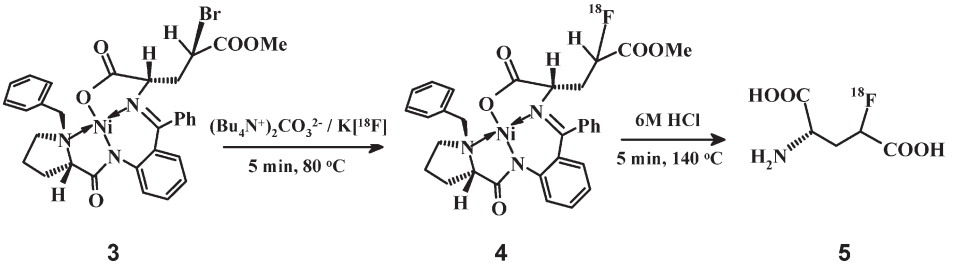

[a] See text for details.

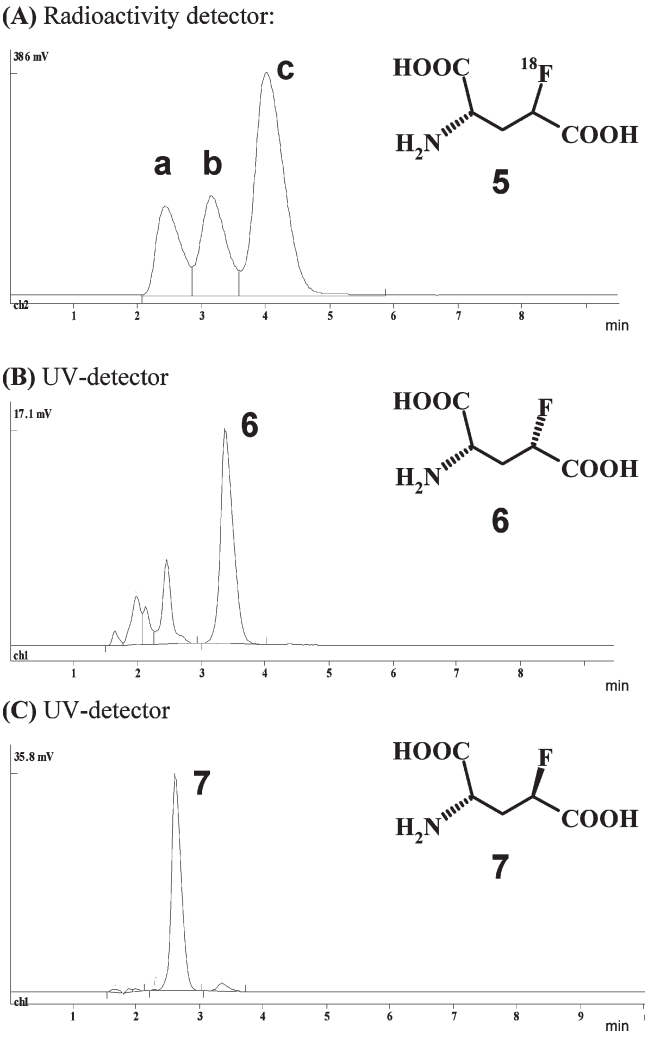

Figure 3. (A) Chiral radiochromatogram of the purified **5** (Crownpak CR (+), Daicel, 150 mm × 4 mm, $HClO_4$ pH 1, 0.8 mL/min, 210 nm) for peak assignment. (B, C) UV detection of cold (2*S*,4*S*)-**6** and (2*S*,4*R*)-**7** after chiral chromatography. Radioactive peak c could be assigned to the (2*S*,4*S*) stereoisomer of **5** (t_R = 4.0 min; 58.3%). Peak b was assigned to the (2*S*,4*R*) stereoisomer of **5** (t_R = 3.2 min; 22.5%). Peak a (unknown, t_R = 2.4 min; 19.2%) could not be assigned yet.

adopted to generate **5** (BAY 85-8050) for subsequent first in vitro characterization.

Results and Discussion

The synthesis route for **5** is outlined in Scheme 1. The Ni^{II} complex of the Schiff base BPB and (2*S*,4*R*)-4-bromoglutamic acid (Ni^{II}-(*S*)-BPB-(2*S*,4*R*)-4-Br-Glu) was used as a chiral auxiliary for the nucleophilic displacement of bromine in the 4-position of the Ni-bound N,O-protected glutamic acid backbone with [^{18}F]fluoride.[17−19] ^{18}F-incorporation was followed by an acidic N,O-deprotection with hydrochloric acid. The resulting **5** was subsequently purified by semipreparative HPLC. The non-carrier-added (nca) nucleophilic fluorination of **3** (Ni^{II}-(*S*)-BPB-(2*S*,4*R*)-4-Br-Glu) was accomplished in acetonitrile at 80 °C in the presence of tetrabutylammonium carbonate (TBAC) as a phase transfer catalyst (PTC). Interestingly, no ^{18}F−Br displacement occurred in the presence of Kryptofix (K2.2.2), a commonly used PTC for nucleophilic substitution reactions.[15]

A detailed outline of the preparation of the activated ^{18}F-complex with Kryptofix 2.2.2. and/or TBAC was published previously.[17] Briefly, an amount of 3.0−5.5 mg of **3** was used in radiofluorinations with TLC monitoring. An aliquot of the reaction mixture was quenched with water and applied to radio-TLC. The resulting chromatogram showed only two peaks, one for the free [^{18}F]fluoride and one for the ^{18}F labeled intermediate (**4**), respectively. ^{18}F-incorporation yields were evaluated based on the TLC data and defined as the ratio of ^{18}F-labeled intermediate over total ^{18}F radioactivity. Usually radiofluorination yields depend on the amounts of residual water in the reaction mixture as already published.[15] This effect had a strong influence on the fluorination yields of the precursor **3**. Thorough removal of residual water from the QMA cartridge retaining the [^{18}F]fluoride was achieved by helium flushing for 15 min, resulting in a ^{18}F fluorine incorporation yield of 75.0% ± 4.1 (n = 9). Attempts to prepare **5** via nucleophilic isotopic exchange of fluorine (^{19}F) in the Ni^{II}-(*S*)-(BPB)-(2*S*,4*S*)-4-F-Glu or Ni^{II}-(*S*)-(BPB)-(2*S*,4*R*)-4-F-Glu precursors by activated [^{18}F]fluoride (Kryptofix K2.2.2 method) failed.

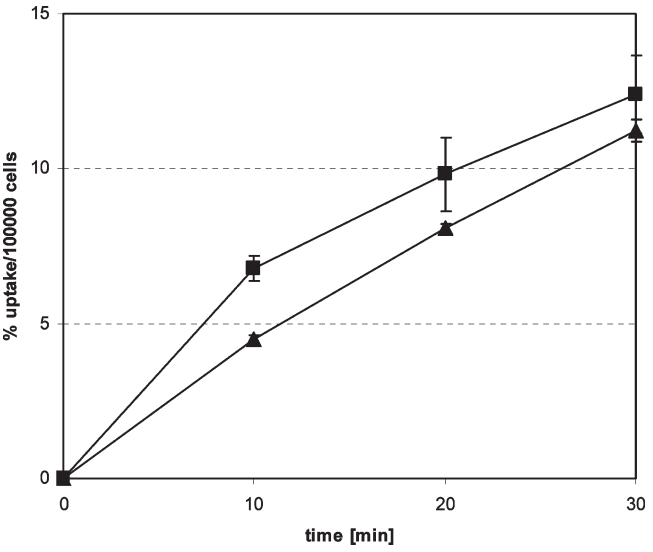

Figure 4. Time dependent uptake of **5** (■) and **1** (▲). Cells were incubated with 250 kBq/well each for the time indicated ($x \pm$ SD, n = 3).

The release of labeled **5** from the ^{18}F Ni-complex intermediate **4** was performed in a single step reaction in aqueous hydrochloric acid. Therefore, concentrations of 1, 2, 4, and 6 M HCl were tested. The use of 6 M HCl proved to be best suited with a yield of 90−96% within 5 min, monitored by radio-TLC. The harsh deprotection conditions did not result in a defluorination side reaction. The crude product **5** was subsequently neutralized and chromatographed on a semipreparative HPLC with a retention time (t_R) of 13 min.

The identity of **5** was confirmed by co-injection of the corresponding [^{19}F] sample (Figure 2) in an isomeric mixture of (2*S*,4*S*)-4-[^{19}F]F-Glu (**6**) and (2*S*,4*R*)-4-[^{19}F]F-Glu (**7**) epimers. Subsequently, a chiral HPLC was applied to assign the stereoisomers (Figure 3) using **6** and **7** as reference compounds.

Three radioactive peaks were observed on the chiral HPLC chromatogram with a major peak (58.3%) assigned to the 2*S*,4*S* isomer of **5**. Its formation as the major product can be attributed to a SN-2 type reaction of bromine in the precursor **3**, with ^{18}F leading to a complete stereochemical conversion.[15] The presence of (2*S*,4*R*)-**5** (22.5%) indicates the occurrence of a partial retention of the configuration at carbon 4. This epimerization in α-position of the carboxylic methyl ester occurs probably because of the harsh acidic conditions of the

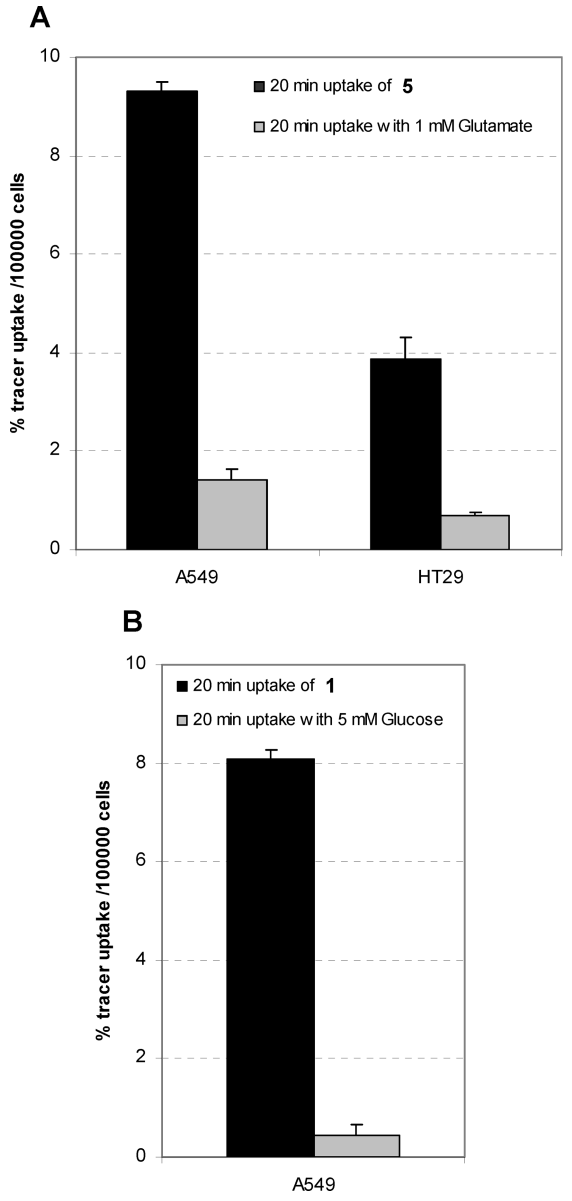

Figure 5. Specificity of uptake. (A) To demonstrate specificity, the uptake of **5** in A549 and HT29 cells was examined using co-incubation with an excess of cold L-glutamic acid (L-Glu, 1 mM). (B) In comparison, competition experiments with A549 cells were performed using **1** and 5 mM D-glucose ($x \pm$ SD, $n = 3$).

deprotection step. A third, not yet identified product (19.2%) was also detected. Further studies are currently ongoing to confirm the total configuration of this species.

Biological Characterization. Tumor cell uptake of the diastereomeric mixture of **5** was investigated in the human lung cancer cell line A549 using adherently growing cancer cells. **1** was used as reference compound and was investigated under analogous conditions. The uptake of **5** in the A549 cells was time dependent as demonstrated in Figure 4. Within 30 min of incubation up to 12% of the applied dose was taken up by the A549 tumor cells. Similar results were obtained for **1** in the same cell line: 11% of applied **1** was taken up by the tumor cells in 30 min (Figure 4). In addition, tumor cell uptake was also performed with the isolated isomers [^{18}F]**6** and [^{18}F]**7** (for results see Supporting Information). As no significant difference in uptake was observed, the diastereomeric mixture of **5** was used for additional experiments.

Uptake of **5** was examined in A549 cells and the colon tumor cell line HT29 in parallel. After 20 min of incubation in assay buffer, 9.3% of the applied dose was taken up in A549 cells and 4% was taken up in HT29 tumor cells, respectively. To demonstrate specificity of tracer uptake, tumor cells were co-incubated with an excess of the corresponding cold compound. Tracer uptake of **5** was reduced in both cell lines by approximately 90% by co-incubation with an excess of L-glutamic acid (1 mM) (Figure 5A). Similarly, uptake of **1** in A549 cells after 20 min was reduced by $>90\%$ by co-incubation with 5 mM D-glucose (Figure 5B). Hence, like **1**, **5** is specifically transported in the tumor cells.

Conclusions

The nucleophilic ^{18}F−Br exchange on a Ni^{II} complex of a Schiff base of (*S*)-BPB with (2*S*,4*R*)-4-bromoglutamic acid as a precursor was successfully adapted to the synthesis of the new ^{18}F-labeled amino acid PET radiotracer, **5**. The synthesis comprises established steps such as tetrabutylammonium carbonate mediated nucleophilic fluorination followed by acid hydrolysis/deprotection and was further adapted to an automated synthesis module. The rapid and specific tumor cell uptake of **5** in the lung and colon cancer cell lines, comparable to **1**, emphasizes the potential of such fluorinated amino acid PET tracers for tumor targeting. Further evaluation of this promising tracer candidate is ongoing in vitro and in vivo.

Experimental Section

General ^{18}F-Labeling Procedure. The labeling precursor **3** was synthesized according to Belokon et al.[19] An amount of 3.0−5.5 mg of precursor **3** was dissolved in 0.5 mL of anhydrous acetonitrile. This solution was added through a Teflon rubber septum into a vial containing the dry [^{18}F]fluorinating agent. The mixture was heated at 80 °C for 5 min without stirring. An aliquot of the mixture was removed with a syringe, quenched with water, and analyzed by radio-TLC (SiO_2 plate, eluent EtOAc/$CHCl_3$/CH_3COOH (4/1/1); R_f [^{18}F]fluoride, 0.1; R_f [^{18}F]intermediate, 0.45. The acetonitrile was removed in a nitrogen flow, and 0.5 mL of aqueous 6.0 M HCl was added following heating at 140 °C for 5 min. An aliquot of the crude reaction mixture was analyzed by radio-TLC (SiO_2 plate, eluent *n*-BuOH/CH_3COOH/H_2O/EtOH (4/1/1.6/0.5)); R_f [^{18}F]fluoride, 0.1; R_f of **5**, 0.51.

Semipreparative HPLC Purification. The crude reaction mixture was cooled and neutralized by adding 0.4 mL of 2.0 M NaOH and 0.4 mL of water to give a total volume of 2 mL. The resulting solution was injected onto the HPLC loop with a motor-driven 5 mL disposable plastic syringe. HPLC separation conditions were as follows: semipreparative Zorbax NH_2 column (9.4 mm × 250 mm, 5 μm); mobile phase, aqueous 0.01 M NaH_2PO_4 (pH 3.5)/ethanol (95/5); flow rate 3.0 mL/min; UV 210 nm. The radioactive fraction containing **5** eluted between 12 and 14 min and was collected into a 10 mL sterile sealed vial. Finally, the solution was passed through a sterile filter (0.22 μm pore size, Millipore, Waters), adjusted to pH 7.4 with PBS buffer, and used for further biological in vitro examination.

Quality Control. The radiochemical purity of **5** was determined to be 97% by TLC (SiO_2 plate, eluent *n*-BuOH/CH_3COOH/H_2O/EtOH (4/1/1.6/0.5); R_f [^{18}F]fluoride, 0.1; R_f **5**, 0.51) and 98% by HPLC (column Zorbax NH_2, 4.6 mm × 250 mm, eluent 10 mM NaH_2PO_4 (pH 3.5)/MeOH (85/15 v/v), 1.5 mL/min).

Acknowledgment. We are grateful to Jana Hannig and Ingo Horn for technical assistance.

Supporting Information Available: Detailed procedures and biological methods. This material is available free of charge via the Internet at http://pubs.acs.org.

References

(1) Warburg, O.; Posener, K.; Negelein, E. Ueber den stoffwechsel der carcinomzelle. *Biochem. Z.* **1924**, *152*, 309–344.

(2) Warburg, O. On the origin of cancer cells. *Science* **1956**, *123*, 309–314.

(3) Kelloff, G. J. Progress and promise of [^{18}F]FDG-PET imaging in cancer patient management and oncologic drug development. *Clin. Cancer Res.* **2005**, *11* (8), 2785–2808.

(4) Hautzel, H.; Muller-Mattheis, V.; Herzog, H.; Roden, W.; Coenen, H. H.; Ackermann, R.; Muller-Gartner, H. W.; Krause, B. J. The (^{11}C) acetate positron emission tomography in prostatic carcinoma. New prospects in metabolic imaging. *Urologe A* **2002**, *41* (6), 569–576.

(5) Machtens, S.; Boerner, A. R.; Hofmann, M.; Knapp, W. H.; Jonas, U. Positron emission tomography (PET) for diagnosis and monitoring of treatment for urological tumors. *Urologe A* **2004**, *43* (11), 1397–1409.

(6) Ide, M. Cancer screening with [^{18}F]FDG-PET. *Q J. Nucl. Med. Mol. Imaging* **2006**, *50* (1), 23–27.

(7) Hess, E.; Sichler, S.; Kluge, A.; Coenen, H. H. Synthesis of 2-[^{18}F]fluoro-L-tyrosine via regiospecific fluoro-de-stannylation. *Appl. Radiat. Isot.* **2002**, *57*, 185–191.

(8) Pauleit, D.; Stoffels, G.; Bachofner, A.; Floeth, F. W.; Sabel, M.; Herzog, H.; Tellmann, L.; Jansen, P.; Reifenberger, G.; Hamacher, K.; Coenen, H. H.; Langen, K. J. Comparison of ^{18}F-FET and ^{18}F-[18F]FDG PET in brain tumors. *Nucl. Med. Biol.* **2009**, *36* (7), 779–787.

(9) Rau, F. C.; Weber, W. A.; Wester, H. J.; Herz, M.; Becker, I.; Kruger, A.; Schwaiger, M.; Senekowitsch-Schmidtke, R. *O*-(2-[(18)F]Fluoroethyl)-L-tyrosine (FET): a tracer for differentiation of tumour from inflammation in murine lymph nodes. *Eur. J. Nucl. Med. Mol. Imaging* **2002**, *29*, 1039–1046.

(10) Lee, T. S.; Ahn, S. H.; Moon, B. S.; Chun, K. S.; Kang, J. H.; Cheon, G. J.; Choi, C. W.; Lim, S. M. Comparison of ^{18}F-[^{18}F]FDG, ^{18}F-FET and ^{18}F-FLT for differentiation between tumor and inflammation in rats. *Nucl. Med. Biol.* **2009**, *36*, 681–686.

(11) Kuhajda, F. P. Fatty acid synthase and cancer: new application of an old pathway. *Cancer Res.* **2006**, *66* (12), 5977–5980.

(12) Swinnen, J. V.; Brusselmans, K.; Verhoeven, G. Increased lipogenesis in cancer cells: new players, novel targets. *Curr. Opin. Clin. Nutr. Metab. Care* **2006**, *9* (4), 358–365.

(13) Costello, L. C.; Franklin, R. B. 'Why do tumour cells glycolyse?': from glycolysis through citrate to lipogenesis. *Mol. Cell. Biochem.* **2005**, *280*, 1–8.

(14) Mazurek, S.; Eigenbrodt, E. The tumor metabolome. *Anticancer Res.* **2003**, *23* (2A), 1149–1154.

(15) Coenen, H. H. Fluorine-18 Labeling Methods: Features and Possibilities of Basic Reactions. In *PET Chemistry: The Driving Force in Molecular Imaging*; Schubiger, P. A., Lehmann, L., Friebe, M., Eds.; Ernst Schering Research Foundation Workshop, 62; Springer-Verlag: Berlin, Germany, 2007; pp15−50.

(16) Hamacher, K.; Coenen, H. H. Efficient routine production of the ^{18}F-labelled amino acid *O*-2-^{18}F-fluoroethyl-L-tyrosine. *Appl. Radiat. Isot.* **2002**, *57*, 853–856.

(17) Krasikova, R. N.; Kuznetsova, O. F.; Fedorova, O. S.; Maleev, V. I.; Savel'eva, T. F.; Belokon, Y. N. No carrier added synthesis of *O*-(2′-[^{18}F]fluoroethyl)-L-tyrosine via a novel type of chiral enantiomerically pure precursor, Ni^{II} complex of a (*S*)-tyrosine Schiff base. *Bioorg. Med. Chem.* **2008**, *16*, 4994–5003.

(18) Belokon, Y. N.; Maleev, V. I.; Saveleva, T. F.; Moskalenko, M. A.; Pripadchev, D. A.; Khrustalev, V. N.; Vorontsov, E. V.; Sagiyan, A. S.; Babayan, E. P. Diastereoselective addition of an Ni^{II} complex of a Schiff base of glycine with (*S*)-2-[*N*-(*N*-benzylprolyl)-amino]benzophenone to the C=C bond of ethyl α-bromoacrylate. *Russ. Chem. Bull. Int. Ed.* **2005**, *54*, 981–987.

(19) Belokon, Y. N.; Maleev, V. I.; Saveleva, T. F.; Moskalenko, M. A.; Pripadchev, D. A.; Khrustalev, V. N.; Sagiyan, A. S. Asymmetric synthesis of enantiomerically and diasteroisomerically enriched 4-[F or Br]-substituted glutamic acids. *Amino Acids* **2010**, *39*, 1171–1176.